Preprints of the 19th World Congress
The International Federation of Automatic Control
Cape Town, South Africa. August 24-29, 2014

Nonlinear Model Predictive Control of a PEM Fuel Cell System for Cathode Exhaust Gas Generation

M. Schultze*, C. Hähnel*, J. Horn*

** Helmut-Schmidt-University/University of the Federal Armed Forces Hamburg, Department of Electrical Engineering, Institute of Control Engineering, Holstenhofweg 85, 22043 Hamburg, Germany (e-mail: martin.schultze@hsu-hh.de)*

Abstract: Polymer electrolyte membrane (PEM) fuel cells are highly efficient energy converters and provide electrical energy, cathode exhaust gas with low oxygen concentration and water. They are investigated as replacement for auxiliary power units (APU) that are currently used for electrical power generation on aircraft. For generation of oxygen depleted cathode exhaust air (ODA) oxygen concentration must be 10-11%. A challenging task is controlling the fuel cell system for this product and simultaneously keeping fuel cell stack degradation, voltage losses and stack damage as low as possible as well as keeping the system within operational limitations such as bounds and gradients on control parameters. This constrained control task for PEM fuel cell systems is attacked by a nonlinear model predictive control (NMPC) strategy. Simulation and experimental results are shown.

Keywords: Nonlinear Model Predictive Control, PEM Fuel Cell System, Aircraft Application.

1. INTRODUCTION

Aircraft are becoming more and more electric as technology relying on electrical power has developed at high pace (McLaughlin, 2009). During ground operations electrical power on aircraft is provided by an auxiliary power unit (APU), which is a significant source of CO_2 as well as noise. PEM fuel cells are very efficient energy converters and are the most suitable for dynamic applications. They are investigated for use on aircraft in a multifunctional manner (Vredenborg et al., 2010). Besides electrical energy, they provide oxygen depleted cathode exhaust air (ODA) for tank-inerting purposes. Oxygen concentration in ODA-gas must not exceed 12% to prevent inflammable fuel vapors (Friedrich et al., 2009) and should stay between 10-11% (Kallo, 2010). Thus far, PEM fuel cell systems have been studied for electrical power supply of autonomous robots (Niemeyer, 2009) or for automotive applications (Pukrushpan et al., 2004), (Karnik et al., 2009). Operation of PEM fuel cell systems for inerting has not yet been studied in detail and is central topic of this paper. Proper fuel cell system operation such as keeping the membrane well hydrated and to proper supply fuel and air as oxygen carrier is a central aspect (Pukrushpan et al., 2004), (Borup et al., 2007). The system studied has an anode recirculation loop for efficient use of hydrogen fuel and for humidification. Water separation in the recirculation loop prevents anode flooding, which is more likely to occur than cathode flooding as cathode gas flow continuously removes cathode water (McKay et al., 2005). Fuel and air supply as well as cooling temperature gradient across the stack is managed by an internal fuel cell system controller. The stack is connected to an ohmic load. Figure 1 shows a schematic of the multifunctional fuel cell system with dehumidifying section consisting of a condenser and water separators (Sep. 1, 2). Oxygen excess ratio termed stoichiometry u_{stoic}, stack current I_{stack}, stack cooling system valve position u_{valve_OL} and reference value $T_{cool\_c,ref}$ for the condenser cooling inlet temperature T_{cool_c} are the fuel cell system inputs $u=[I_{stack}, T_{cool\_c,ref}, u_{stoic}, u_{valve\_OL}]^T$. Condenser cooling inlet temperature T_{cool_c} is controlled for separately.

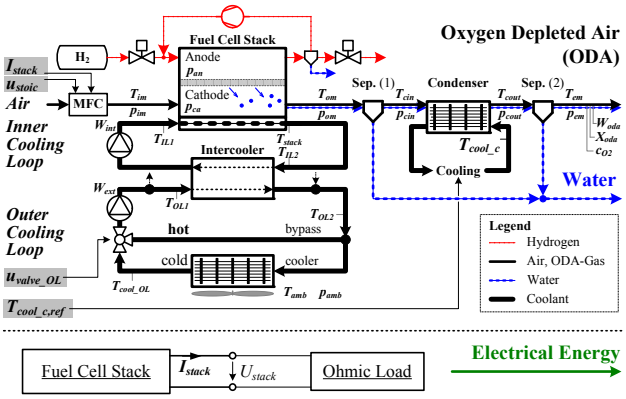

Fig. 1. Schematic of the fuel cell system comprising stack, separators (Sep.1, 2), condenser, inlet-, outlet- and exit manifold (im, om, em), condenser and stack cooling system with intercooler and cooling valve; H2 is recirculated.

For controlling the fuel cell system for ODA-gas mass flow, operational limitations such as bounds and gradient on stack current and bounds on condenser cooling temperature have to be satisfied. A suitable approach is model predictive control due to its inherent capability of incorporating constraints. Model predictive control (MPC) has been successfully applied to fuel cell systems for electrical power supply (Niemeyer, 2009). In a preliminary simulation study MPC was applied to control for ODA-gas mass flow and stack cooling temperature (Schultze et al., 2013a). To keep computational burden low, stack cooling control is managed by a separate cooling controller. This paper presents a real-time capable nonlinear model predictive control strategy based on a sequential quadratic programming (SQP)

approach (Grüne and Pannek, 2011) to control the fuel cell system for ODA-gas generation. The system model is briefly outlined in section 2. Fuel Cell System Model. The nonlinear model predictive control (NMPC) strategy is presented in section 3. NMPC Strategy. Simulation and experimental results are shown in Section 4. Simulation and Experimental Results.

2. FUEL CELL SYSTEM MODEL

The fuel cell system model comprises the fuel cell stack cathode and anode and a controlled air-valve for cathode feed air supply (mass flow controller, MFC). A thin polymer membrane with high water diffusivity separates cathode from anode. Due to the membrane's high diffusivity, stack humidification is maintained as long as stack temperature, gas flow through cathode and load change gradient stay within operational limits. Under these assumptions, a perfectly hydrated membrane can be assumed. The MFC delivers a cathode feed air mass flow as specified by actual stoichiometry and stack current. However, it may deliver slightly too much flow in order to allow for fast air delivery. This behavior leads to a higher ODA-gas mass flow than expected and results in an ODA-gas oxygen concentration rise as more oxygen is fed to the cathode. Stack temperature is managed by an internal controller operating stack cooling pump, whereas reference temperature difference across the stack $\Delta T_{stack,ref}$ is a function of system inputs. ODA-gas and inlet air are modeled as ideal gases with inlet air considered dry and consisting of 21% (vol.) oxygen (O_2) and 79% nitrogen (N_2). When limiting stack current slope sufficiently, oxygen starvation and cathode flooding can be prevented to avoid serious dynamic voltage losses. With the previous assumptions a reduced order model is derived. The model captures two major dynamics: gas and thermal dynamics. Model states are as follows and y the model output with X_{oda} being the ODA-gas water loading.

$$\begin{aligned} \underline{x} &= \begin{bmatrix} W_{mfc} & W_{oda} & c_{O2} & z_{mfc} & T_{stack} & T_{IL1} \dots \\ \dots T_{IL2} & T_{OL1} & T_{OL2} & T_{cool\_OL} & T_{cool\_c} \end{bmatrix}^T \\ \dot{\underline{x}} &= \underline{f}(\underline{x},\underline{u}) \qquad y = h(\underline{x}) = X_{oda} \end{aligned} \tag{1}$$

1.1 Fuel Cell System Gas Dynamics

Pressure in the volumes establishes fast as compared to the remaining system dynamics and therefore is modeled as static (Niemeyer, 2009). Pressure depends on the gas mass flow through the fuel cell system. Cathode feed air mass flow is provided by the MFC, whose dynamics are described by a first order time system with time constant T_{mfc}. Gas flow dynamics through the inlet manifold, cathode and the downstream volumes such as outlet manifold, condenser and exit manifold are grouped together and are modeled as a first order time system with time constant T_{FC}. A disturbance mass flow z_{mfc} accounts for the feed air mass flow deviation. Measurement of the oxygen concentration c_{O2} is a relatively slow process and is captured by a first order time system with time constant T_{O2}. The gas states are as follows with W_{mfc} the mass flow provided by the MFC, W_{oda} the ODA-gas mass flow leaving the fuel cell system and z_{mfc} the mass flow disturbance of the MFC. Model equations for the gas dynamics are stated by (2). Cathode feed air mass flow is the sum of W_{mfc} and z_{mfc} and a mass flow $I_{stack}n_{cells}M_{O2}/(4F)$ of O_2 is consumed by the chem. reaction $4H^+ + O_2 + 4e^- \rightarrow 2H_2O$.

$$\frac{dW_{mfc}}{dt} = \frac{1}{T_{mfc}}\left(I_{stack}u_{stoic}\frac{n_{cells}}{4F}\left(M_{O2} + \frac{0.79}{0.21}M_{N2} \right) - W_{mfc} \right) \tag{2a}$$

$$\frac{dW_{oda}}{dt} = \frac{1}{T_{FC}}\left(W_{mfc} + z_{mfc} - I_{stack}\frac{n_{cells}}{4F}M_{O2} - W_{oda} \right) \tag{2b}$$

$$\frac{dc_{O2}}{dt} = \frac{1}{T_{O2}}\left(\frac{N_{O2out}}{N_{O2out} + N_{N2out}} - c_{O2} \right) \tag{2c}$$

$$\frac{dz_{mfc}}{dt} = 0 \tag{2d}$$

Oxygen concentration is determined by O_2 molar flow N_{O2out} and nitrogen molar flow N_{N2out} leaving the stack (3). Both flows are determined by O_2 mass fraction of air x_{O2} and molar masses M_{O2} for O_2 and M_{N2} for N_2. Oxygen inlet flow is reduced by the consumption during chemical reaction. Cathode feed air mass flow is determined as sum of W_{mfc} and z_{mfc}. Number of cells in stack is n_{cells}. F is Faraday constant.

$$\begin{aligned} N_{O2out} &= \frac{1}{M_{O2}}x_{O2}\left(W_{mfc} + z_{mfc}\right) - \frac{I_{stack}}{4F}n_{cells} \\ N_{N2out} &= \frac{1}{M_{N2}}\left(1 - x_{O2}\right)\left(W_{mfc} + z_{mfc}\right) \end{aligned} \tag{3}$$

1.2 Fuel Cell System Thermal Dynamics

Thermal dynamics cover stack cooling system, condenser cooling system and ODA-gas water loading, which depends on temperature and pressure. The stack cooling system's inner cooling loop is filled with coolant of specific heat capacity c_{int} and is being pumped at cooling mass flow W_{int}. The outer loop coolant is being pumped at mass flow W_{ext} and has a specific heat capacity c_{ext}. W_{int} is driven by an internal controller to satisfy cooling temperature gradient across the stack. Outer loop coolant mass flow is set constant. Both loops are coupled by an intercooler. The intercooler is captured as a static model (Schultze et al., 2012) as the cooling system's thermal mass is higher than the intercooler's thermal mass. Cooling valve position u_{valve_OL} in the outer loop sets the level of mixture of cooler and bypass coolant. This is described by a static model. Thermal states are stack temperature T_{stack}, T_{IL1} and T_{IL2} being the inner loop, T_{OL1} and T_{OL2} being the outer loop cooling temperatures, cooler temperature T_{cool_OL} and condenser cooling inlet temperature T_{cool_c}. Water loading is given by X_{oda} in g/kg. The system schematic in figure 1 depicts the temperature locations. Further parameters for the thermal model are stack heat capacity C_{stack}, coolant masses m_{IL1}, m_{IL2} in the inner loop, m_{OL1}, m_{OL2} and m_c in the outer loop and the cooler as well as time constant T_c of the controlled condenser cooling system, ambient temperature T_{amb} and cooler parameter k_c. A portion of 6% of W_{ext} is taken for hydrogen recirculation pump cooling (Schultze et al., 2012). The coolant temperature rise through the compressor, however, is considered negligible small as the hydrogen compressor generates a low heat flow as compared to the fuel cell stack. Cooling mass flow through the intercooler is modeled as 94% of W_{ext}. The thermal model differential equations are stated below (4a-g).

$$\frac{dT_{stack}}{dt} = \frac{W_{\text{int}} c_{\text{int}}}{C_{stack}} \left(T_{IL1} - T_{stack}\right) + \frac{1}{C_{stack}} \dot{Q}_{FC} \tag{4a}$$

$$\frac{dT_{IL1}}{dt} = \frac{W_{\text{int}}}{m_{IL1}} \left(T_{IL1in} - T_{IL1}\right) \tag{4b}$$

$$\frac{dT_{IL2}}{dt} = \frac{W_{\text{int}}}{m_{IL2}} \left(T_{stack} - T_{IL2}\right) \tag{4c}$$

$$\frac{dT_{OL1}}{dt} = \frac{W_{ext}}{m_{OL1}} \left(u_{valve\_OL} \left(T_{cool\_OL} - T_{OL2}\right) + T_{OL2} - T_{OL1}\right) \tag{4d}$$

$$\frac{dT_{OL2}}{dt} = \frac{W_{ext}}{m_{OL2}} \left(0.94 T_{OL2in} + 0.06 T_{OL1} - T_{OL2}\right) \tag{4e}$$

$$\frac{dT_{cool\_OL}}{dt} = \frac{W_{ext}}{m_c} u_{valve\_OL} \left(T_{OL2} - T_{cool\_OL}\right) - k_c \frac{T_{cool\_OL} - T_{amb}}{m_c c_{ext}} \tag{4f}$$

$$\frac{dT_{cool\_c}}{dt} = \frac{1}{T_c} \left(T_{cool\_c,ref} - T_{cool\_c}\right) \tag{4g}$$

1.3 Intercooler Model

A counter-flow heat exchanger interconnects inner and outer cooling loop. For modeling heat exchangers the effectiveness NTU method (Shah and Sekulic, 2003) has shown very good results. NTU is the number of transfer units, which is an important parameter in heat exchanger design. Outlet temperatures are calculated explicitly on the inlet temperatures and the cooling mass flows. Heat flow is gained by inlet temperature differences, minimum heat capacity flow $C_{min} = min(C_h, C_c)$ and effectiveness e_{NTU}. Temperatures into inner loop T_{IL1in} (5) and into outer loop T_{OL2in} (6) are gained by heat capacity flow of inner $C_h = W_{int} c_{int}$ and outer loop $C_c = 0.94 W_{ext} c_{ext}$. Intercooler inlet temperatures are T_{IL2} and T_{OL1}. Effectiveness e_{NTU} for a counter-flow heat exchanger (Shah and Sekulic, 2003) is given by (7), (8) with UA being the parameter describing the heat transfer.

$$T_{IL1in} = T_{IL2} - \frac{1}{C_h} \left(e_{NTU} C_{\min} \left(T_{IL2} - T_{OL1}\right)\right) \tag{5}$$

$$T_{OL2in} = T_{OL1} + \frac{1}{C_c} \left(e_{NTU} C_{\min} \left(T_{IL2} - T_{OL1}\right)\right) \tag{6}$$

$$C^* = C_{\min} / \max(C_c, C_h), \quad NTU = UA / C_{\min} \tag{7}$$

$$e_{NTU} = \begin{cases} NTU/(1+NTU) & C^* = 1 \\ \dfrac{1 - \exp\left(-NTU\left(1 - C^*\right)\right)}{1 - C^* \exp\left(-NTU\left(1 - C^*\right)\right)} & otherwise \end{cases} \tag{8}$$

1.4 Fuel Cell System Pressure

System pressure is necessary for determining stack heat flow, voltage and ODA-gas water loading. As mentioned previously, pressure establishes fast in comparison to the major system dynamics (Niemeyer, 2009), (Pukrushpan et al., 2004) and therefore is obtained by a static model. It is assumed that pressure changes with ODA-gas mass flow. System pressure is obtained by nonlinear flow equations due to water loading and a turbulent flow regime (Schultze and Horn, 2012). Inlet manifold pressure p_{im} is not required in the following. Pressure vector $p = [p_{ca}, p_{om}, p_{cin}, p_{cout}, p_{em}]^T$ could be computed at once, which however would require an iterative algorithm. An alternative is calculating the pressure vector starting from the last element by inverting the mass flow equations with p_{amb} being ambient pressure. ODA-gas in the exit manifold has a very low water loading due to the dehumidifying section. The nonlinear flow is gained by $W_{oda} = k_{em} \sqrt{p_{em} - p_{amb}}$. Exit manifold pressure is obtained by equation (9) with k_{em} being the flow constant. ODA-flow at the condenser exit is considered to carry a low vapor mass flow due to the low temperature. Therefore, pressure p_{cout} (10) at the condenser outlet is gained equivalently to p_{em}.

$$p_{em} = \left(W_{oda} / k_{em}\right)^2 + p_{amb} \tag{9}$$

$$p_{cout} = \left(W_{oda} / c_{sep2}\right)^2 + p_{em} \tag{10}$$

At the condenser inlet the ODA-gas flow is assumed to be fully saturated at nearly stack temperature and thus has a high water loading. The temperature at condenser inlet, which is assumed to be outlet manifold temperature T_{om}, is gathered by $T_{om} = T_{stack} - \Delta T_{om}$ with ΔT_{om} accounting for ODA-gas cooling. The change of water loading across the upstream separator (sep. 1) is negligible small leading to the assumption that water loading X_{om} in the outlet manifold equals the one at the condenser inlet. The nonlinear flow is gained as (11) with flow constant c_{sep1} and c_c for the separator and the condenser, respectively.

$$\begin{aligned} \left(1 + X_{om}\right) W_{oda} &= c_{sep1} \sqrt{p_{om} - p_{cin}} \\ \left(1 + X_{om}\right) W_{oda} &= c_c \sqrt{p_{cin} - p_{cout}} \end{aligned} \tag{11}$$

$$X_{om} = p_v^{sat}\left(T_{om}\right) / \left(p_{om} - p_v^{sat}\left(T_{om}\right)\right) \cdot R_{oda} / R_v \tag{12}$$

Comparing equations (11) with each other leads to (13) determining outlet manifold pressure p_{om}. Inserting equation (13) into (12) leads to (14) that is an equation of one unknown p_{cin}, which is solved by the iterative regula-falsi method "Illinois Algorithm" (Ford, 1995).

$$p_{om} = p_{cin} + \left(c_c / c_{sep1}\right)^2 \left(p_{cin} - p_{cout}\right) \tag{13}$$

$$0 = c_c \sqrt{p_{cin} - p_{cout}} - \left(1 + X_{om}\right) W_{oda} \tag{14}$$

Flow equation for the fully saturated gas flow with high water loading leaving the cathode is given by equation (16). Cathode pressure p_{ca} is determined iteratively as done for p_{cin}.

$$\begin{aligned} 0 &= k_{ca} \left(p_{ca} - p_{om}\right) - \left(1 + X_{ca}\right) W_{oda} \\ X_{ca} &= p_v^{sat}\left(T_{stack}\right) / \left(p_{ca} - p_v^{sat}\left(T_{stack}\right)\right) \cdot R_{oda} / R_v \end{aligned} \tag{16}$$

Liquid water resides in the cathode, hence fully saturated gas is assumed there. Dry gas cathode pressure is obtained by subtracting vapor saturation pressure from p_{ca}. Cathode O_2 partial pressure (17) is gained by applying O_2 molar fraction $c_{ca,O2} = N_{O2out} / (N_{O2out} + N_{N2out})$ with flows of equation (3).

$$p_{ca,O2} = c_{ca,O2} \left(p_{ca} - p_v^{sat}\left(T_{stack}\right)\right) \tag{17}$$

1.5 Fuel Cell Voltage and Fuel Cell Stack Heat Flow

Stack voltage depends on stack current, temperature, oxygen partial pressure and on membrane humidity (O'Hayre et al., 2009), (Amphlett et al., 1995). The membrane is assumed perfectly hydrated due to its thinness. This motivates reducing the humidity dependent membrane resistance (O'Hayre et al., 2009) to a constant ohmic resistance R_{ohm}. Reversible cell voltage U_{rev} depends on hydrogen partial pressure. Motivated by the anode pressure control (Niemeyer, 2009), a constant hydrogen partial pressure p_{H2} is assumed.

Stack voltage U_{stack} is the sum of all cell voltages U_{cell}, which is modeled as $U_{cell} = U_{rev} - \eta_{act} - \eta_{ohm}$ as follows (18). Parameters $\zeta_1, \ldots \zeta_4$ and R_{ohm} have been identified by a least square error minimization using experimental data.

$$\begin{aligned} U_{rev} &= 1.229 - 0.85 \cdot 10^{-3}(T_{stack} - 298.15) + 4.3 \cdot 10^{-5} T_{stack}\left(\ln\frac{p_{H2}}{p_0} + \frac{1}{2}\ln\frac{p_{O2}}{p_0}\right) \\ \eta_{act} &= \zeta_1 + \zeta_2 T_{stack} + \zeta_3 T_{stack} \ln\left(p_{O2} e^{(498/T_{stack})} / 5.08 \cdot 10^{-6}\right) + \zeta_4 T_{stack} \ln(I_{stack}) \\ \eta_{ohm} &= R_{ohm} I_{stack} \end{aligned} \tag{18}$$

The stack heat flow is the sum of heat flow generated by the chemical reaction and caused by the fluid flows in the stack. It is assumed that liquid water is produced by the reaction and partially evaporates in the stack. Hence, higher heating value (HHV) of hydrogen is assumed. Water leaves the stack as liquid and vapor. H_2 chemical energy flow reduced by stack electrical power leads to the chemical reaction heat flow (19).

$$\dot{Q}_{reaction} = (n_{cells}\, HHV/(2F) - U_{stack}) I_{stack} = (n_{cells} 1.48V - U_{stack}) I_{stack} \tag{19}$$

$$\begin{aligned} \dot{Q}_{flow} = &\left((W_{mfc} + z_{mfc}) c_{air} T_{im}\right) \\ &- \left(W_{oda} c_{oda} T_{stack} + W_v (h_0 + c_v T_{stack}) + W_l c_l T_{stack}\right) \end{aligned} \tag{20}$$

$$\dot{Q}_{fc} = \dot{Q}_{reaction} + \dot{Q}_{flow} \tag{21}$$

Heat flow transported by the fluids (20) is a static model with c_{air}, c_{oda}, c_v, c_l being the specific heat capacities of air, ODA, vapor and water as well as h_0 being the enthalpy of evaporation. Inlet manifold temperature T_{im} is set constant. Heat is transported by inlet air, ODA-gas flow, vapor and liquid water. A water mass flow of $W_{H2O} = M_{H2O}/(2F) n_{cells} I_{stack}$ is generated by the reaction. Water evaporates until it reaches vapor saturation pressure or until all water available has evaporated, which is accounted for by modeling vapor mass flow as $W_v = min(W_{H2O}, X_{ca} W_{oda})$ with X_{ca} as in equation (16) and liquid mass flow gained by $W_l = W_{H2O} - W_v$. Heat flows (19) and (20) result in the fuel cell stack heat flow (21).

1.6 Inner Loop Coolant Mass Flow, ODA-Gas water loading

An internal PI controller adjusts the inner loop cooling pump leading to a temperature difference $\Delta T_{stack} = T_{stack} - T_{IL1}$ across the stack matching the reference $\Delta T_{stack,ref}$. W_{int} measurement signal is not available online. Evolution of W_{int} is captured by a static model (22) derived from a stationary energy balance across the stack. W_{int} is limited to minimum $W_{int,min}$ and maximum $W_{int,max}$ by $W_{int} = min(max(W_{int,ref}, W_{int,min}), W_{int,max})$.

$$W_{\mathrm{int},ref} = \dot{Q}_{fc} / \left(c_{\mathrm{int}} \Delta T_{stack,ref}\right) \tag{22}$$

Both water separators in the dehumidifying section exhibit very high separation rates, which are modeled as 100% efficient. As only vapor and ODA-gas leave the downstream separator, water loading X_{oda} in g/kg is determined as follows (23). Due to very high cooling capacity, ODA-gas is cooled to almost cooling inlet temperature T_{cool_c}. Therefore, exit manifold temperature T_{em} at which ODA-gas leaves the condenser is modeled as $T_{em} = T_{om} - e_{NTU,c}(T_{om} - T_{cool\_c})$ with effectiveness $e_{NTU,c} = 1$. Besides temperature, condensation depends on pressure, which is modeled as the arithmetic mean of condenser inlet and outlet pressure p_{cin} and p_{cout}.

$$X_{oda} = \frac{p_v^{sat}(T_{em})}{\frac{1}{2}(p_{cin} + p_{cout}) - p_v^{sat}(T_{em})} \frac{R_{oda}}{R_v} \times 1000 \tag{23}$$

3. NMPC STRATEGY

In model predictive control (MPC) a finite horizon open-loop optimal control problem is solved online for every sampling time step and yields an optimal control sequence from which the first sequence is applied. Current system state, which is obtained by measurement or estimation, serves as initial state. MPC's major advantage is handling constraints on states and inputs (Mayne et al., 2000). MPC is based on linear constraints and a linear model describing the system dynamics. Nonlinear model predictive control (NMPC) refers to MPC schemes being applied to nonlinear constraints and nonlinear models describing system dynamics (Allgöwer et al., 2004). NMPC problems generally cannot be solved analytically, calling for numerical algorithms. Optimal control problems can be solved by dynamic programming, direct and indirect methods. In dynamic programming the computational cost grows with the problem's dimension (Kirk, 2004). Its application is limited to problems with low order such as the energy-optimal control of a car (Back, 2005). Indirect methods are based on the first order optimality conditions of calculus of variations and involve solving a two-point boundary value problem, which may require significant effort or is impossible for complex systems (Aburajabaltamimi, 2011). NMPC problems are widely solved by direct methods that convert the optimal control problem into a nonlinear programming problem, which is solved iteratively by a sequential quadratic programming (SQP) method. Inequality constraints can easily be included. In this method a quadratic program is solved for the linearized optimization problem and linearized constraints. A comprehensive overview over NMPC is given in (Grüne and Pannek, 2011). This paper presents an NMPC strategy solved by an SQP method.

$$\begin{aligned} \dot{\underline{x}}_{nmpc}(t) &= \underline{f}_{nmpc}\left(\underline{x}_{nmpc}(t), \underline{u}_{nmpc}(t), T_{IL1}(t)\right) \\ \underline{x}_{nmpc}(t) &= \left[W_{mfc} \quad W_{oda} \quad c_{O2} \quad z_{mfc} \quad T_{stack} \quad T_{cool\_c}\right]^T \\ y_{nmpc}(t) &= h_{nmpc}\left(\underline{x}_{nmpc}\right) = X_{oda} \end{aligned} \tag{24}$$

The system model $\underline{f}_{nmpc}$ for the NMPC algorithm leaves out the stack cooling system dynamics (4b)-(4f) as these are controlled for by a separate cooling controller. Stack cooling inlet temperature T_{IL1} is now considered a constant input to the model. The model equations reduce to the set (24). Control input $\underline{u}_{nmpc}(t) = [u_{1,0} \quad u_2 \quad u_{stoic}]^T$ with constant stoichiometry u_{stoic}, stack current $u_{1,0}$ and condenser cooling reference temperature u_2 is applied. Values $u_{1,0}$ and u_2 are the first control values of the NMPC algorithm solution vector.

In real-time environments control inputs are applied at constant time intervals. Result $\underline{u}_{nmpc}(t)$ of NMPC algorithm started at time instance t is applied at the next time instance $t+T_s$ as shown in figure 2. Hence there is a delay of one sampling period between the initial condition $\underline{x}_{nmpc}(t)$ gained by measurement or state estimation and application of the NMPC result. An estimate of the correct time initial condition $\hat{\underline{x}}_{nmpc}(t+T_s)$ is gained by a prediction taking $\underline{x}_{nmpc}(t)$ and the present time control input $\underline{u}_{nmpc}(t-T_s)$. Prediction involves time-integrating the system equations using a 4th order Runge-Kutta scheme with constant step size (25).

$$\hat{\underline{x}}_{nmpc}(t+T_s) = \underline{x}_{nmpc}(t) + \int_t^{t+T_s} \underline{f}_{nmpc}\left(\underline{x}_{nmpc}(\tau), \underline{u}_{nmpc}(t-T_s), T_{IL1}(t)\right) d\tau \tag{25}$$

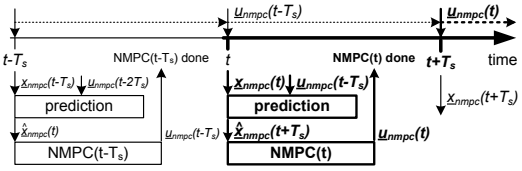

Fig. 2. NMPC strategy for real-time application with prediction for an estimate of the NMPC initial condition

2.1 NMPC problem formulation

An algorithm for tracking ODA-gas mass flow and leading to minimum ODA-gas water loading is presented below. To prevent cathode flooding or oxygen starvation the stack current gradient is bounded (26) to limit load change gradient and to minimize dynamic stack voltage losses. Limitations on gradient of stack current $dI_{stack,max}$ are assumed symmetric. Stack current is bounded to $I_{stack,min}$ and $I_{stack,max}$ to keep the fuel cell system within its operational limits. Condenser cooling inlet temperature reference is bounded by an upper limit $T_{cool\_c,max}$ and a minimum limit of max(5°C, $T_{cool\_c,amb}$) to prevent freezing inside the condenser. Ambient cooling temperature $T_{cool\_c,amb}$ sets a minimum possible temperature.

$$\begin{aligned} -dI_{stack,\max} &\le \frac{dI_{stack}}{dt} \le dI_{stack,\max} \\ I_{stack,\min} &\le I_{stack} \le I_{stack,\max} \\ \max\left(5, T_{cool\_c,amb}\right) &\le T_{cool\_c,ref} \le T_{cool\_c,\max} \end{aligned} \tag{26}$$

The optimal control problem is discretized into N time steps with sampling time step length T_s=*500ms*. Prediction horizon is $N*T_s$. Two independent control variables would lead to *2N* variables to be solved for. To keep the number of variables low, the slow condenser cooling system dynamics are exploited and $T_{cool\_c,ref}$ stays constant over the whole prediction horizon. So, the vector $\underline{u}_{opt} = [u_{1,0}\ u_{1,1} \ldots u_{1,k} \ldots u_{1,N-1}\ u_2]^T$ with the optimization variables has length $N+1$. Only the instances $u_{1,0}$ and u_2 of the optimal control sequence are applied. The optimal control problem is turned into a nonlinear programming problem by discretization of (24) through time-integration over prediction horizon $N\,T_s$. Time-integration leads to N+1 state vectors including the initial condition $\underline{x}_{nmpc,k}=[x_{nmpc,k}(1)\ x_{nmpc,k}(2) \ldots x_{nmpc,k}(6)]^T$ with $n_{states}=6$ states and N+1 outputs $y_{nmpc,k}$. Time integration is done by a 4th order Runge-Kutta method with constant step size (27).

$$\begin{aligned} \underline{x}_{nmpc,k+1} &= \underline{x}_{nmpc,k} + \int_{kT_s}^{(k+1)T_s} \underline{f}_{nmpc}\left(\underline{x}_{nmpc}(\tau), \left[u_{1,k}\ \ u_2\ \ u_{stoic}\right]^T, T_{IL1}(t)\right) d\tau \\ y_{nmpc,k} &= h_{nmpc}\left(\underline{x}_{nmpc,k}\right) \qquad \left(\underline{x}_{nmpc,0} = \hat{\underline{x}}_{nmpc}\left(t+T_s\right),\ \ k = 0,1,\ldots N-1\right) \end{aligned} \tag{27}$$

The nonlinear minimization problem is stated as follows (28).

$$\min_{\underline{u}_{opt}} J\left(\underline{u}_{opt}\right) \tag{28a}$$

$$\begin{aligned} J\left(\underline{u}_{opt}\right) = {} & q_{11}\left(x_{nmpc,N}(2) - x_{2,ref}\right)^2 + q_{12}\left(y_{nmpc,N}(5)^2 + \ldots\right. \\ & + T_s \sum_{k=0}^{N-1} \left[q_{21}\left(x_{nmpc,k}(2) - x_{2,ref}\right)^2 + q_{22}\left(y_{nmpc,k}\right)^2 + \ldots \right. \\ & \left. \left. + q_{23}\left(u_{1,k} - u_{1,ref}\right)^2 + q_{24}\left(u_2\right)^2 \right] \end{aligned} \tag{28b}$$

$$\begin{aligned} \underline{k=0:} \quad & u_1^* - dI_{stack\,\max} T_s \le u_{1,k} \le u_1^* + dI_{stack\,\max} T \\ \underline{k=1..N-1:} \quad & -dI_{stack\,\max} T_s \le u_{1,k} - u_{1,k-1} \le +dI_{stack\,\max} T_s \end{aligned} \tag{28c}$$

$$\begin{aligned} I_{stack,\min} &\le u_{1,k} \le I_{stack,\max} \\ \max\left(5, T_{cool\_c,amb}\right) &\le u_2 \le T_{cool\_c,\max} \end{aligned} \tag{28d}$$

It is subject to system dynamics (27) and constraints (28c-d). Objective function $J(\underline{u}_{opt})$ (28b) to be minimized (28a) gains state vector $\underline{x}_{nmpc,k}$ from (27). It combines tracking control of ODA-gas mass flow for reference value $x_{2,ref}$ by simultaneously requiring low ODA-gas water loading. Input variables are penalized to prevent their heavy use. Weighing factors q_{11}, q_{12}, q_{21}…,q_{24} influence balance between control performance and accuracy in steady state. (Morari et al., 2012) show that steady state accuracy can be achieved by introducing an input reference gained by steady state analysis of the system model with disturbances. To improve steady state accuracy but also to prevent nonlinear effects due to incorporation of noisy disturbances, stack current reference $u_{1,ref}$ (29) based on a stationary analysis of (1a) and (1b) requiring $W_{oda}=x_{2,ref}$ and $z_{mfc}=0$ is introduced in (28b). Optimization objective J (28b) consists of a Lagrange term ($k=0, 1 \ldots N-1$) for transient behavior and a terminal penalty term ($k=N$) (Allgöwer et al., 2004). NMPC needs $N \geq 2$ for a working algorithm (Grüne and Pannek, 2011).

$$u_{1,ref} = 4F \Big/ \left(n_{cells} \left(M_{O2}\left(u_{stoic} - 1\right) + u_{stoic} \frac{0.79}{0.21} M_{N2} \right) \right) x_{2,ref} \tag{29}$$

The linear gradient inequality constraints (26) are discretized by finite differences leading to the linear inequality constraints for the input variables u_1 (28c). Values u_1^* are the optimal control sequence of the last NMPC run. Lower and upper bounds on the optimization variables are derived from (26) and applied for every time instant k (28d).

NMPC requires the entire state $\underline{x}_{nmpc}(t)$ as initial condition for the nonlinear programming problem. It is assumed that the state vector can be measured perfectly or estimated and is available at present time. The nonlinear optimization problem (28) is solved by SOLNP (Ye, 1989). For faster convergence of the iterative SQP algorithm the solution vector of the present step is taken for construction of the optimization initial condition for the next step as follows $[u_{1,1} \ldots u_{1,k} \ldots u_{1,N-1}\ u_{1,N-1}\ u_2]^T$. The first element $u_{1,0}$ is discarded and the last element $u_{1,N-1}$ is taken twice. Value u_2 is initialized as max(5°C, $T_{cool\_c,amb}$) to gain minimum water loading.

4. SIMULATION AND EXPERIMENTAL RESULTS

The NMPC strategy based on the model (24) was applied to the plant model (1). Disturbance mass flow z_{mfc} is set 0 constantly. There is no model/plant mismatch in this simulation study. The simulation study was performed with constant weighing parameters and was started from steady state for every trial. Stack cooling inlet temperature reference is 58°C and stoichiometry was set to u_{stoic}= 1.7 for every trial to gain 10% ODA-gas oxygen content. Figure 3 shows the results for runs with $u_{1,ref}$=0 and $u_{1,ref}$ set to improve steady state accuracy. Reference for W_{oda} is 0.1 and 0.167 g/s/cell. Stack current gradient is limited to $dI_{stack,max}$=0.0125A/s/I_{max}. As shown in figure 3 steady state accuracy of the ODA-gas mass flow improves significantly by using the control input reference value in the objective function. The simulation shows only a minor deviation of ODA-gas water loading between the runs which is due to the mass flow and hence system pressure differences. As there is no disturbance acting, ODA-gas oxygen content stays close to 10%. This NMPC algorithm finishes within the sampling time of 500ms

and thus is applicable for real-time application as validated by experiments shown in figure 4 performed with the parameters used for the simulation study and with $u_{1,ref}$ set. An Unscented Kalman Filter algorithm presented in (Schultze et al., 2013b) is used for fuel cell system state estimation. Despite disturbances on the real plant the mass flow is controlled for very accurately. Due to mass flow disturbances and as stoichiometry is kept at u_{stoic} =1.70, oxygen content increases to a value greater than 10% but still less than 11%. The NMPC algorithm keeps the operational limitations.

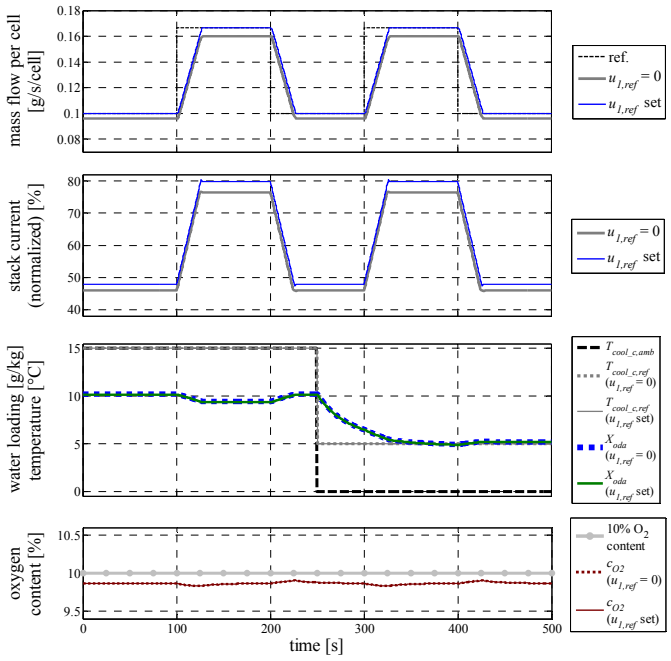

Fig. 3. Simulation results: ODA-gas mass flow scaled to n_{cells} (top); stack current normalized (2nd from top); condenser cooling reference temperature, ODA-gas water loading (3rd from top) and O_2 content (bottom) for $u_{1,ref}$=0 and $u_{1,ref}$ set

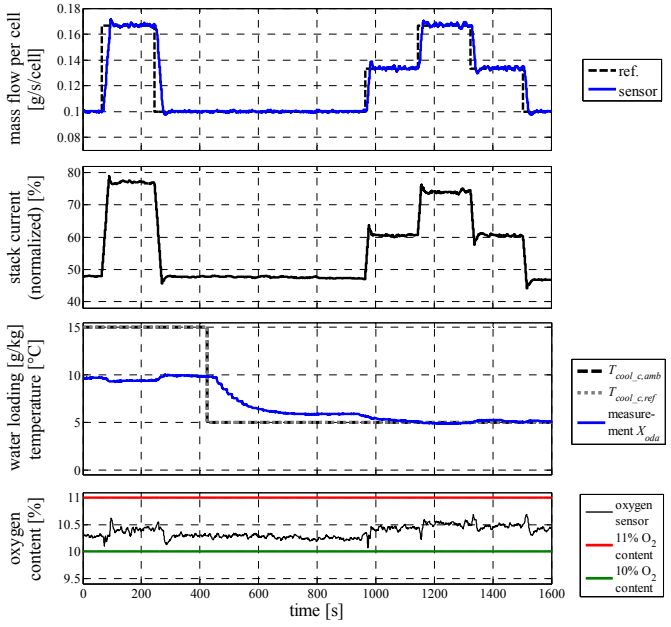

Fig. 4. Experimental results: ODA-gas mass flow per cell (top), stack current normalized (2nd from top), ODA-gas water loading (3rd from top) and oxygen content (bottom)

5. CONCLUSIONS

A nonlinear model predictive control (NMPC) strategy for the control of a PEM fuel cell system for oxygen depleted air production is developed and presented in this paper. The NMPC strategy includes inequality constraints to satisfy operational limitations of the fuel cell system. The optimization problem is attacked by an iterative SQP method and solved within the sampling time. The NMPC algorithm has been applied to simulation and experiments at the real plant. Results are shown.

ACKNOWLEDGMENT

This study as part of the project “cabin technology and multifunctional fuel cell systems” has been supported by Airbus and the German Federal Ministry of Education and Research (support code: 03CL03A).

REFERENCES

Aburajabaltamimi, J. (2011), Development of Efficient Algorithms for Model Predictive Control of Fast Systems, Dissertation, Fakultät für Informatik und Automatisierung, Technische Universität Ilmenau, Ilmenau, 10 January.

Allgöwer, F., Findeisen, R. and Nagy, Z.K. (2004), Nonlinear Model Predictive Control: From Theory to Application, *Journal of Chinese Institute of Chemical Engineers*, Vol. 35 No. 3, pp. 299–315.

Amphlett, J.C., Baumert, R.M., Mann, R.F., Peppley, B.A. et al. (1995), Performance Modeling of the Ballard Mark IV Solid Polymer Electrolyte Fuel Cell I. Mechanistic Model Development, *Journal of the Electrochemical Society*, Vol. 142 No. 1, pp. 1–8.

Back, M. (2005), Prädiktive Antriebsregelung zum Energieoptimalen Betrieb von Hybridfahrzeugen, Dissertation, Fakultät für Elektrotechnik und Informationstechnik, Universität Karlsruhe, Karlsruhe, 2005.

Borup, R., Meyers, J., Pivovar, B., Kim, Y.S., Mukundan, R. et al. (2007), Scientific aspects of polymer electrolyte fuel cell durability and degradation, *Chemical Reviews*, Vol. 107 No. 10, pp. 3904–3951.

Ford, J.A. (1995), Improved Algorithms of Illinois-type for the Numerical Solution of Nonlinear Equations, *Technical Report CSM-257, University of Essex Press*.

Friedrich, K.A., Kallo, J., Schirmer, J. and Schmitthals, G. (2009), Fuel Cell Systems for Aircraft Applications, *ECS Transactions*, Vol. 25 No. 1, pp. 193–202.

Grüne, L. and Pannek, J. (2011), *Nonlinear Model Predictive Control: Theory and Algorithms*, Springer, London.

Kallo, J., Renouard-Vallet, G., Saballus, M., Schmithals, G., Schirmer, J. and Friedrich, K.A. (2010), Fuel Cell System Development and Testing for Aircraft Applications, *18th World Hydrogen Energy Conference 2010 – WHEC 2010*, 16-21 May 2010

Karnik, A.Y., Sun, J., Stefanopoulou, A.G. and Buckland, J.H. (2009), Humidity and Pressure Regulation in a PEM Fuel Cell Using a Gain-Scheduled Static Feedback Controller, *IEEE Transactions on Control Systems Technology*, Vol. 17 No. 2.

Kirk, D.E. (2004), *Optimal Control Theory: An Introduction*, Dover Publications.

Mayne, D.Q., Rawlings, J.B., Rao, C.V. and Scokaert, P.O.M. (2000), Constrained model predictive control: Stability and optimality, *Automatica*, Vol. 36 No. 6, pp. 789–814.

McKay, D.A., Ott, W. and Stefanopoulou, A.G. (2005), Modeling, Parameter Identification and Validation of Reactant and Water Dynamics for a Fuel Cell Stack, *ASME 2005 International Mechanical Engineering Congress and Exposition*, pp. 1177–1186.

McLaughlin, A. (2009), More Electric - Ready for take off?, *EPE '09, 13th European Conference on Power Electronics and Applications, 2009* 8-10 September 2009, pp. 1–7.

Morari, M. and Maeder, U. (2013), Nonlinear offset-free model predictive control, *Automatica*, Vol. 48, pp. 2059-2067.

Niemeyer, J. (2009), Modellprädiktive Regelung eines PEM-Brennstoffzellensystems, Dissertation, University of Karlsruhe, Karlsruhe, 2009.

O'Hayre, R., Cha, S.-W., Colella, W. and Prinz, F.B. (2009), *Fuel Cell Fundamentals*, John Wiley & Sons, Inc., Hoboken, NJ.

Pukrushpan, J.T., Stefanopoulou, A.G. and Peng, H. (2004), *Control Of Fuel Cell Power Systems: Principles, Modeling, Analysis, And Feedback Design,* 1st ed., Springer, London.

Schultze, M. and Horn, J. (2012), Optimization Approach for Cathode Exhaust Gas Conditioning of a Multifunctional PEM Fuel Cell System for the Application in Aircraft, *Deutscher Luft- und Raumfahrtkongress 2012, Berlin* urn:nbn:de:101:1-201211163965.

Schultze, M., Kirsten, M., Helmker, S. and Horn, J. (2012), Modeling and simulation of a coupled double-loop-cooling system for PEM-fuel cell stack cooling, *2012 UKACC International Conference on Control* 3-5 Sept. 2012, pp. 857–863.

Schultze, M. and Horn, J. (2013a), Nonlinear Model Predictive Control of PEM Fuel Cell Systems for Generation of Exhaust Gas with Low Oxygen Content, *19th IFAC Symposium on Automatic Control in Aerospace*, 2-6 September 2013.

Schultze, M. and Horn, J. (2013b), State Estimation for PEM Fuel Cell System with Time Delay by an Unscented Kalman Filter and Predictor Strategy, *21st Mediterranean Conference on Control & Automation*, 25-28 June 2013.

Shah, R.K. and Sekulic, D.P. (2003), *Fundamentals of Heat Exchanger Design*, John Wiley & Sons, Inc., Hoboken, NJ.

Vredenborg, E., Lüdders, H. and Thielecke, F. (2010), Methodology for Sizing and Simulation of complex Fuel Cell Systems orig.(german) Methodik zur Auslegung und Simulation Komplexer Brennstoffzellensysteme, *Deutscher Luft- und Raumfahrtkongress 2010.*

Ye, Y. (1989), *SOLNP Users' Guide - A Nonlinear Optimization Program in Matlab.*